Charm spectroscopy from amplitude analyses in B(s) decays at LHCb

Melissa Cruz Torres[1,2] on behalf of the LHCb collaboration

[1] *Universidad Nacional Autónoma de Honduras (UNAH), Honduras*
[2] *Centro Brasileiro de Pesquisas Físicas (CBPF), Brazil*

June 2nd, 2021

Introduction

- Charm meson spectroscopy is of great interest, theoretically and experimentally, as a testing ground for quark-models predictions in the Standard Model.

Production of conventional and exotic charm states from B-decays

- Well defined initial state
- Low background
- Kinematics constraint

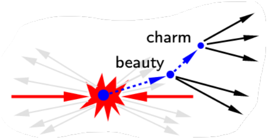

Exotic measurements through amplitude analysis techniques

- Dalitz plot is the visual representation of the phase space
- Perform fits as function of the phase space variables
- Two kinematics variables m_{12}^2, m_{23}^2

- Complex phases and magnitudes can be extracted (interference of resonance)
- Lineshapes and spin can be extracted

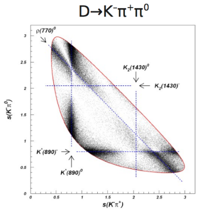

Image credit: Brian Meadows

The LHCb Experiment

- It is a single-arm forward spectrometer designed for the study of B and D mesons.
- It covers a pseudo-rapidity range of $2 < \eta < 5$
- run I data: $\mathcal{L} = 3.0\ \text{fb}^{-1}$ from pp collisions at 7 TeV (2011) and 8 TeV (2012) in the center-of-mass-energy
- run II data: $\mathcal{L} = 6.0\ \text{fb}^{-1}$ from pp collisions at 13 TeV (2015-2018)

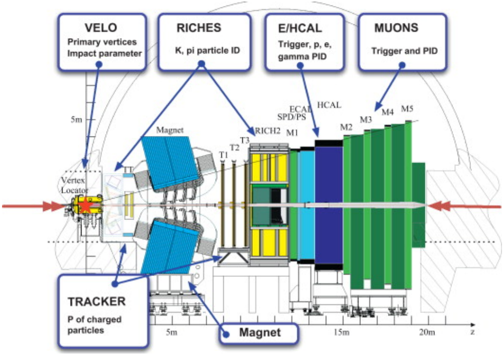

Int. J. Mod. Phys A 30, 1530022 (2015)

Outline

- **Observation of a new excited D_s^+ meson in $B^0 \to D^- D^+ K^+ \pi^-$ decays**
  - $\mathcal{L} = 5.4$ fb^{-1}, run II data from 2016 to 2018, Phys. Rev. Lett. 126 (2021) 122002
- **Determination of quantum numbers for several excited charmed mesons observed in $B^- \to D^{*+}\pi^-\pi^-$**
  - $\mathcal{L} = 4.7$ fb^{-1}, run I 2011+2012 and run II 2015+2016 data , Phys. Rev. D101 (2020) 032005
- **Amplitude analysis of $B^+ \to D^+ D^- K^+$ decays**
  - $\mathcal{L} = 9$ fb^{-1}, run I 2011 + 2012 and run II 2015 to 2018 data , Phys. Rev. D102 (2020) 112003
- **Model-independent studies of $B^+ \to D^+ D^- K^+$ decays**
  - $\mathcal{L} = 9$ fb^{-1}, run I 2011 + 2012 and run II 2015 to 2018 data , Phys. Rev. Lett. 125 (2020) 242001

Observation of a new excited D_s^+ meson in $B^0 \to D^- D^+ K^+ \pi^-$ decays

Phys. Rev. Lett. 126 (2021) 122002

Motivation

- The study of the charm-strange spectrum is rich in structures $\Rightarrow$ interesting place for testing theories.

  - Some states are already experimentally well established
  - **But some predicted states are still not observed**

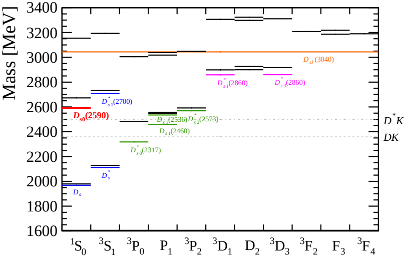

- **The 2^1S_0 state** $\Rightarrow$ Predicted as the radial excitation of the pseudoscalar D_s^+ state; the lightest with mass around 2.6 GeV.
- **Two *D*-wave states** (mass around 2.86 GeV): $1^3D_2(2^-)$ and $1^1D_2(2^-)$
- **Three *P*-wave states** with mass around 3 GeV: $2^3P_0(0^+)$, $2^1P_1(1^+)$ and $2^3P_2(2^+)$

meson states - $n^{2S+1}L_J$, spin-parity - J^P

Observation of a new excited D_s^+ meson in $B^0 \to D^- D^+ K^+ \pi^-$ decays

Motivation

- D_s states has been observed in $B \to D\bar{D}K$ decays [Phys.Rev.Lett.100(2008)092001]
- Most studies has been focused in excited D_s^+ decaying into DK
  - Only sensitive to D_s^+ natural spin-parity states.
- The $D^+ K^+ \pi^-$ allows to access all spin-parity D_s states in a large mass range
  - If restricted the $K\pi$ system to a low mass region (below the threshold of the $K^*(892)^0$), then only the D_s^+ resonance with unnatural spin-parity ($J^P = 0^-, 1^+, 2^-, \ldots$) can decay into $DK\pi$.
  - **Offers the possibility to search for the missing $D_s(2S)$ state, with mass around 2.6 GeV and $J^P = 0^-$.**

Observation of a new excited D_s^+ meson in $B^0 \to D^- D^+ K^+ \pi^-$ decays

Extraction of the signal and background yields from unbinned maximum likelihood fit [Phys. Rev. Lett. 126 (2021) 122002], run II data 2016 to 2018.

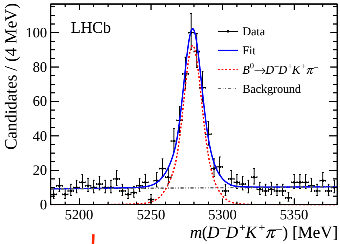

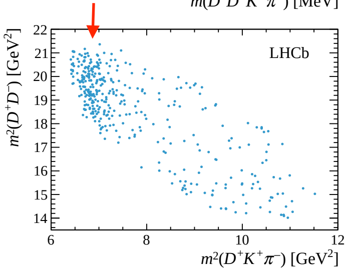

- Fit to the B^0 spectrum in the low $K^+\pi^-$ region ($m(K\pi) < 0.75$ GeV)
- 444 ± 27 B^0 signal candidates

Dalitz plot in the square mass of $D^+ D^-$ vs $D^+ K^+ \pi^-$

- For candidates with masses within 20 MeV of the known B^0 mass
- **Clear cluster of candidates** observed in the $D^+ K^+ \pi^-$ mass $\approx$ **2.6 GeV**
  - ▷ **Excess of data!**
- Small peak at the threshold correspond $D_{s1}(2536)^+$ state.

Observation of a new excited D_s^+ meson in $B^0 \to D^- D^+ K^+ \pi^-$ decays

- To study the structures in the $D^+ K^+ \pi^-$ system an amplitude analysis is performed in the low $K^+ \pi^-$ mass region. Amplitude constructed using the Helicity formalism

Decay chain: $B^0 \to \bar{D} D_{sJ}$, $D_{sJ} \to D K_n^*$, $K_n^* \to K\pi$.

- **Three D_s^+ components with unnatural spin-parity considered:**
  - A new D_{sJ}^+ state at 2.6 GeV (three hypothesis: $0^-, 1^+$ and 2^+)
  - The $J^P = 1^+ D_{s1}(2536)^+$ state
  - A $J^P = 0^-$ nonresonant (NR) component

- **For the $K^+ \pi^-$ system**
  - Modeled by $J^P = 0^+ K_0^*(700)^0$ for all three D_s^+ components.

D_{sJ}^+, $K_0^*(700)^0$ and $D_{s1}(2536)^+$ are described by relativistic Breit-Wigner functions

Best fit results: $J^P = 0^-$ projections in the $DK\pi$ and $K\pi$ systems and $cos(\theta_{Ds})$

Phys. Rev. Lett. 126 (2021) 122002

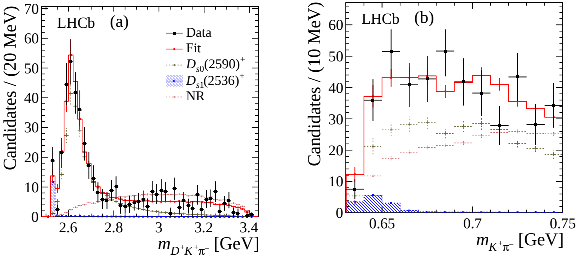

	Fit fraction ($\times 10^{-2}$)
$D_{s0}(2590)^+$	63 ± 9 (stat) ± 9 (syst)
$D_{s1}(2536)^+$	3.9 ± 1.4 (stat) ± 0.8 (syst)
NR	51 ± 11 (stat) ± 19 (syst)
D_{s0}^+ –NR	−18 ± 18 (stat) ± 24 (syst)
D_{s1}^+ / D_{s0}^+	6.1 ± 2.4 (stat) ± 1.4 (syst)

- Best fit with D_{sk}, $J^P = 0^-$
- mass = 2591 ± 6 ± 7 MeV
- Γ= 89 ± 16 ± 12 MeV

D_{sk}, $J^P = 0^- \rightarrow D_{s0}(2590)^+$

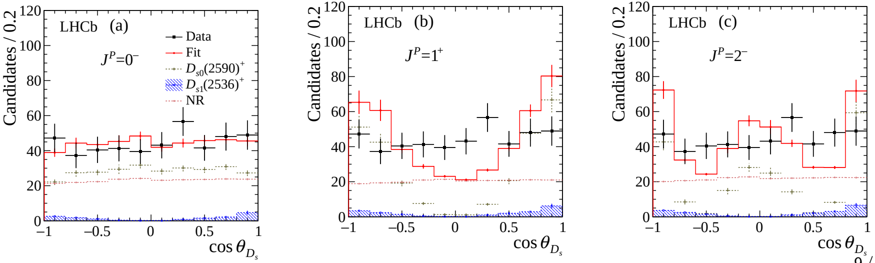

Summary

Phys. Rev. Lett. 126 (2021) 122002

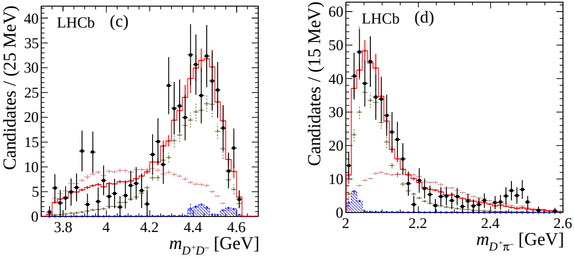

- High mass in D^+D^- and low mass $D^+\pi^-$ are well described as reflections of $D_{s0}(2590)^+$.

- A new excited D_s^+ meson is observed in the $D^+K^+\pi^-$ system of $B^0 \to D^-D^+K^+\pi^-$ decays.
  - From amplitude analysis performed in the low $K^+\pi^-$ region:
    - $m = 2591 \pm 6 \pm 7$ MeV
    - $\Gamma = 89 \pm 16 \pm 12$ MeV
    - $J^P = 0^-$
- The new resonance, denoted as $D_{s0}(2590)^+$, is a good candidate to be the missing $D_s(2^1S_0)^+$ state $\Rightarrow$ the radial excitation of the pseudoscalar D_s^+ meson.

- **Determination of quantum numbers for several excited charmed mesons observed in $B^- \to D^{*+}\pi^-\pi^-$**
    - $\mathcal{L} = 4.7$ fb^{-1}, run I 2011+2012 and run II 2015+2016 data, Phys. Rev. D101 (2020) 032005

Determination of quantum numbers for several excited charmed mesons observed in $B^- \to D^{*+}\pi^-\pi^-$

Phys. Rev. D101 (2020) 032005

- Spin-parity information is crucial to associate observed and predicted resonances
- $D\pi$ final states enables a search for natural spin-parity resonances $J^P = 0^+, 1^-, 2^+,...,$ labeled as D^*
- $D^*\pi$ spectrum enables for both, natural and unnatural spin-parity resonances $J^P = 0^-, 1^+, 2^-,...,$ indicated as D
  - Search for excited mesons, D_J, performed using two different approached:
  - Using inclusive reactions
  - Through amplitude analysis of exclusive B decays

• The amplitude analysis of B decays allows a full spin-parity analysis of charmed mesons.
• Backgrounds are usually low and well understood.

In this work the study of D_J spectroscopy in the $D^{*+}\pi^-$ system through an amplitude analysis of the decay channel $B^- \to D^{*+}\pi^-\pi^-$ is performed

Determination of quantum numbers for several excited charmed mesons observed in $B^- \to D^{*+}\pi^-\pi^-$

Phys. Rev. D101 (2020) 032005

The decay tree proceed as:
$B^- \to R^0\pi_2^-$, where $R^0 \to D^0\pi^+\pi_1^-$

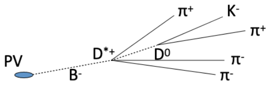

The $B^- \to D^{*+}\pi^-\pi^-$ invariant mass after selection

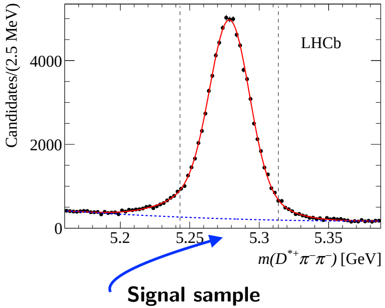

Spectrum after multivariate selection to remove combinatorial background.

Signal candidates

- $N_{sig} = 79120$ where 48.5% and 51.5% are from run I and run II, respectively.

The $B^- \to D^{*+}\pi^-\pi^-$ Dalitz plot

• Two indistinguishable π^- mesons in the final states. Dalitz plot constructed in the $m^2(D^{*+}\pi^-)_{high}$ and $m^2(D^{*+}\pi^-)_{low}$ variables (Phys. Rev. D101 (2020) 032005)

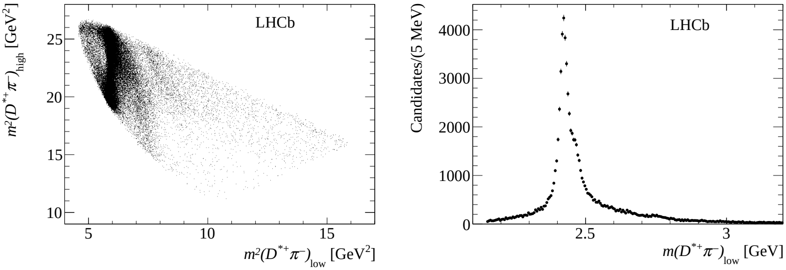

• Clear vertical bands in the 6 GeV^2 mass ⇒ presence of well known $D_1(2420)$ and $D_2^*(2460)$ resonances

• Presence of further weaker bands at higher mass region ⇒ Not so visible in the mass projection and thus, an angular analysis needed to separate the different contributions.

The $B^- \to D^{*+}\pi^-\pi^-$ Amplitude Analysis

An amplitude analysis to extract:

- fractions and phases of the charmed resonances contributing to the decay
- Measure their parameters and quantum numbers.

The contributing amplitudes are parametrized using the nonrelativistic Zemach tensor formalism:

J^P	L	Amplitude
0^-	1	$\mathrm{BW}(m_{123})[\boldsymbol{t_3} \cdot \boldsymbol{p_3}]$
1^+S	0	$\mathrm{BW}(m_{123})[\boldsymbol{t_3} \cdot \boldsymbol{q_4}]$
1^+D	2	$\mathrm{BW}(m_{123})[\boldsymbol{p_3}(\boldsymbol{t_3} \cdot \boldsymbol{p_3}) - \frac{1}{3}(\boldsymbol{p_3} \cdot \boldsymbol{p_3})\boldsymbol{t_3}] \cdot \boldsymbol{q_4}$
1^-	1	$\mathrm{BW}(m_{123})[(\boldsymbol{t_3} \times \boldsymbol{p_3}) \cdot \boldsymbol{q_4}]$
2^-P	1	$\mathrm{BW}(m_{123})[\frac{1}{2}(t_3^i p_3^j + t_3^j p_3^i) - \frac{1}{3}(\boldsymbol{t_3} \cdot \boldsymbol{p_3})\delta^{ij}] \cdot [q_4^i q_4^j - \frac{1}{3}\lvert q_4\rvert^2 \delta^{ij}]$
2^-F	3	$\mathrm{BW}(m_{123})[(\boldsymbol{t_3} \cdot \boldsymbol{p_3})(p_3^i p_3^j - \frac{1}{3}\lvert p_3\rvert^2 \delta^{ij})] \cdot [q_4^i q_4^j - \frac{1}{3}\lvert q_4\rvert^2 \delta^{ij}]$
2^+	2	$\mathrm{BW}(m_{123})[\frac{1}{2}[(\boldsymbol{t_3} \times \boldsymbol{p_3})^i p_3^j + p_3^i(\boldsymbol{t_3} \times \boldsymbol{p_3})^j] - \frac{1}{3}[(\boldsymbol{t_3} \times \boldsymbol{p_3}) \cdot \boldsymbol{p_3}]\delta^{ij} \cdot [q_4^i q_4^j - \frac{1}{3}\lvert q_4\rvert^2 \delta^{ij}]$
3^-	3	$\mathrm{BW}(m_{123})[(\boldsymbol{t_3} \times \boldsymbol{p_3})^i p_3^j p_3^k + (\boldsymbol{t_3} \times \boldsymbol{p_3})^k p_3^i p_3^j + (\boldsymbol{t_3} \times \boldsymbol{p_3})^j p_3^i p_3^k)$ - $\frac{1}{5}[\delta^{ij}(\boldsymbol{t_3} \times \boldsymbol{p_3})^k + \delta^{ik}(\boldsymbol{t_3} \times \boldsymbol{p_3})^j + \delta^{jk}(\boldsymbol{t_3} \times \boldsymbol{p_3})^i]\lvert p_3\rvert^2]\cdot$ $\frac{1}{5}[(p_4^i p_4^j p_4^k + p_4^k p_4^i p_4^j + p_4^j p_4^i p_4^k) - p_4^2(\delta^{ij} p_4^k + \delta^{ik} p_4^j + \delta^{jk} p_4^i)]$

- List of amplitudes included in the analysis

Phys. Rev. D101 (2020) 032005

The $B^- \to D^{*+}\pi^-\pi^-$ Amplitude Analysis

Strategy

- As a first approach, the resonance (R^0) lineshape is described by a complex relativistic Breit-Wigner function.
- Second approach: the resonance line shapes are described by quasi-model-independent method (QMI)
- Allow mixing between $J^P = 1^+$ amplitudes.

- **Dalitz plot fit**

Likelihood function

$$\mathcal{L} = \prod_{n=1}^{N}\left[p \cdot \epsilon(\boldsymbol{x}_n)\frac{\sum_{i,j} c_i c_j^* A_i(\boldsymbol{x}_n) A_j^*(\boldsymbol{x}_n)}{\sum_{i,j} c_i c_j^* I_{A_i A_j^*}} + (1-p) B(z_n)\right]$$

Fit fractions

$$f_i \equiv \frac{|c_i|^2 \int |A_i(\boldsymbol{x})|^2 \mathrm{d}\boldsymbol{x}}{\sum_{i,j} c_i c_j^* I_{A_i A_j^*}}.$$

- All charmed resonance contributions are included one by one. Resonances are kept if a significant likelihood increase ($\Delta(2\log\mathcal{L}) > 3$) is observed

The $B^- \to D^{*+}\pi^-\pi^-$ Amplitude Analysis

List of resonance used in the amplitude analysis:

Resonance	J^P	Mass [MeV]	Width [MeV]	Significance (σ)
$D_1(2420)$	1^+	$2424.8 \pm 0.1 \pm 0.7$	$33.6 \pm 0.3 \pm 2.7$	
$D_1(2430)$	1^+	$2411 \pm 3 \pm 9$	$309 \pm 9 \pm 28$	
$D_2^*(2460)$	2^+	2460.56 ± 0.35	47.5 ± 1.1	
$D_0(2550)$	0^-	$2518 \pm 2 \pm 7$	$199 \pm 5 \pm 17$	53
$D_1^*(2600)$	1^-	$2641.9 \pm 1.8 \pm 4.5$	$149 \pm 4 \pm 20$	60
$D_2(2740)$	2^-	$2751 \pm 3 \pm 7$	$102 \pm 6 \pm 26$	16
$D_3^*(2750)$	3^-	$2753 \pm 4 \pm 6$	$66 \pm 10 \pm 14$	8.7
D_1	1^+	$2423.7 \pm 0.1 \pm 0.8$	$31.5 \pm 0.1 \pm 2.1$	
D_1'	1^+	$2452 \pm 4 \pm 15$	$444 \pm 11 \pm 36$	

- Upper section: list of of states giving significant contribution in the Dalitz plot fit
- Upper section: parameters using the QMI method
- Results in lower part from the mixing analysis

The $B^- \to D^{*+}\pi^-\pi^-$ Amplitude Analysis

Quasi-Model-Independent amplitude

- 31 slices in the $D^{*+}\pi^-$ spectrum
- The process starts with a QMI fit to the $J^P = 1^+S$ amplitude
- Then QMI $J^P = 1^+S$ amplitude is fixed and the QMI $J^P = 0^-$ performed. The process continue by leaving one by one, free Breit-Wigner parameters for all considered resonance.

The fitted magnitude and phase of the 1^+S amplitude is presented. The red point indicate mass bin where the complex amplitude was fixed.

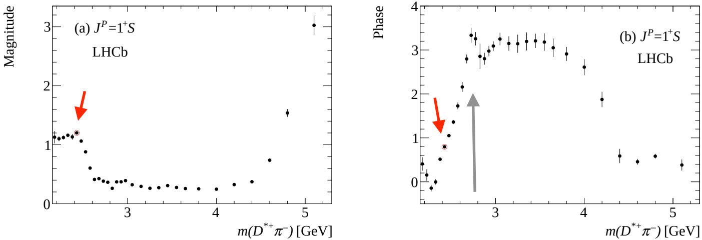

- Broad structure at threshold with corresponding phase motion → (Phys. Rev. D101 (2020) 032005)

The $B^- \to D^{*+}\pi^-\pi^-$ Amplitude Analysis

QMI for $J^P = 0^-$ amplitude

- Fitted amplitude and phase (Phys. Rev. D101 (2020) 032005)

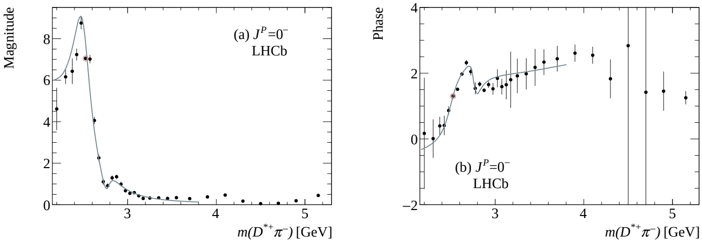

- Activity at 2.8 GeV consistent with a resonance (new excited D_0' resonance)
- Fitted parameters $m(D_0') = 2782 \pm 13$ MeV and $\Gamma(D_0') = 146 \pm 23$ MeV, with 3.2σ of significance.
  - However, an attempt to include this new possible resonance in the amplitude analysis gives a fraction consistent with zero.

The $B^- \to D^{*+}\pi^-\pi^-$ Amplitude Analysis

QMI fit results for $J^P = 1^+S$ and $J^P = 0^-$ amplitudes

Phys. Rev. D101 (2020) 032005

Resonance	J^P	fraction (%)	phase (rad)
→ $D_1(2420)$	1^+D	$59.8 \pm\ 0.3\ \pm 2.9$	0
→ 1^+S QMI	1^+S	$28.3 \pm\ 0.3\ \pm 1.9$	$-1.19 \pm 0.01\ \pm 0.15$
→ $D_2^*(2460)$	2^+	$15.3 \pm\ 0.2\ \pm 0.3$	$-0.71 \pm 0.01\ \pm 0.48$
$D_1(2420)$	1^+S	$2.8 \pm\ 0.2\ \pm 0.5$	$1.43 \pm 0.02\ \pm 0.31$
0^- QMI	0^-	$10.6 \pm\ 0.2\ \pm 0.7$	$1.94 \pm 0.01\ \pm 0.19$
$D_1^*(2600)$	1^-	$6.0 \pm\ 0.1\ \pm 0.6$	$1.20 \pm 0.02\ \pm 0.05$
$D_2(2740)$	2^-P	$1.9 \pm\ 0.1\ \pm 0.4$	$-1.57 \pm 0.04\ \pm 0.15$
$D_2(2740)$	2^-F	$3.2 \pm\ 0.2\ \pm 1.1$	$1.11 \pm 0.04\ \pm 0.29$
$D_3^*(2750)$	3^-	$0.35 \pm 0.04 \pm 0.05$	$-1.17 \pm 0.07\ \pm 0.31$
Sum		$128.2 \pm\ 0.6\ \pm 3.8$	

- Model 1^+S and 0^- with QMI using cubic spline
- All other resonances modeled as relativistic Breit-Wigner amplitudes

- Dominance of $D_1(2420)$ (1^+D) and with important contributions from QMI 1^+S and $D_2^*(2460)$.
- Sum of fractions larger than 100% indicating interference effects.

The $B^- \to D^{*+}\pi^-\pi^-$ Amplitude Analysis

- Fit projections for Run 2 data (Phys. Rev. D101 (2020) 032005):

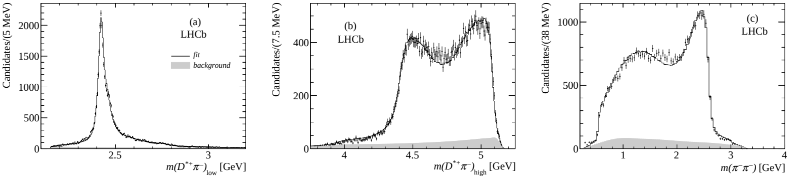

- Fit projections on $m(D^{*+}\pi^-)_{low}$ for all dataset, including all contributing amplitudes:

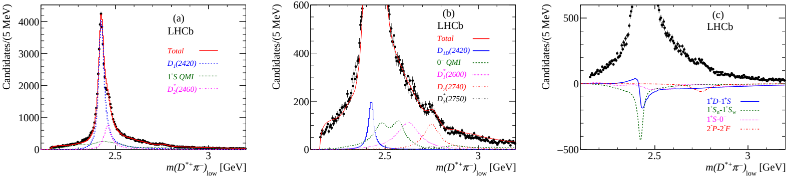

The $B^- \to D^{*+}\pi^-\pi^-$ Amplitude Analysis

- Search for additional contributions and spin-parity determination
  - Additional contributions are tested by adding them to the reference fit.
  - No evidence is found for $D_1^*(2760)$ or $D_2^*(3000)$ contributions previously observed in the $B^- \to D^+\pi^-\pi^-$ decay.
  - Their statistical significance is found to be 2.4 and 0.0, respectively.

Results from the $J^P = 1^+$ mixing model

- The mixing can occur via common $D^*\pi$ decay channel

$$A^{D_1'} = A^{1S}\cos\omega - A^{1D}\sin\omega e^{i\psi},$$

$$A^{D_1} = A^{1S}\sin\omega + A^{1D}\cos\omega e^{-i\psi},$$

- D_1' and D_1 being the superposition of S- and D-wave amplitudes
- ω is the mixing angle and ψ a complex phase

Results Phys. Rev. D101 (2020) 032005

Resonance	J^P	fraction (%)	phase (rad)
D_1	1^+	$58.9 \pm 0.7 \pm 2.5$	0
D_1'	1^+	$21.9 \pm 2.2 \pm 3.0$	$-1.06 \pm 0.10 \pm 0.05$
$D_2^*(2460)$	2^+	$14.0 \pm 0.2 \pm 0.3$	$2.66 \pm 0.09 \pm 0.15$
0^- QMI	0^-	$6.5 \pm 0.2 \pm 1.5$	$2.03 \pm 0.09 \pm 0.28$
$D_1^*(2600)$	1^-	$4.9 \pm 0.1 \pm 0.5$	$-2.24 \pm 0.09 \pm 0.11$
$D_2(2740)$	2^-P	$0.72 \pm 0.08 \pm 0.30$	$-2.59 \pm 0.10 \pm 0.53$
$D_2(2740)$	2^-F	$2.9 \pm 0.2 \pm 1.1$	$0.27 \pm 0.09 \pm 0.47$
$D_3^*(2750)$	3^-	$0.70 \pm 0.05 \pm 0.10$	$1.54 \pm 0.10 \pm 0.33$
Sum		$110.4 \pm 2.3 \pm 4.4$	

The $B^- \to D^{*+}\pi^-\pi^-$ Amplitude Analysis

Results from the $J^P = 1^+$ mixing model

- The resulting mixing parameter are (Phys. Rev. D101 (2020) 032005)

$$\omega = -0.063 \pm 0.019 \pm 0.004,\ \psi = -0.29 \pm 0.09 \pm 0.07$$

- consistent with Belle results (Phys. Rev. D93, 119901(2016)):

$$\omega = -0.010 \pm 0.03 \pm 0.02 \pm 0.02$$
$$\psi = 0.05 \pm 0.20 \pm 0.04 \pm 0.06$$

- The fitted $D_1^{'}$ and D_1 parameters are (Phys. Rev. D101 (2020) 032005)

$$m(D_1) = 2423.7 \pm 0.1 \pm 0.8 \text{ MeV} \quad \text{and} \quad \Gamma(D_1) = 31.5 \pm 0.1 \pm 2.1 \text{ MeV},$$
$$m(D_1^{'}) = 2452 \pm 4 \pm 15 \text{ MeV} \quad \text{and} \quad \Gamma(D_1^{'}) = 444 \pm 11 \pm 36 \text{ MeV}$$

The $B^- \to D^{*+}\pi^-\pi^-$ Amplitude Analysis

Measurements of branching fractions Phys. Rev. D101 (2020) 032005

The known branching fraction of $B^- \to D^{*+}\pi^-\pi^-$ is

$$\mathcal{B}(B^- \to D^{*+}\pi^-\pi^-) = (1.35 \pm 0.22) \times 10^{-3} \text{ (PDG)}$$

- The partial branching fraction is obtained as the multiplication of the B^- branching fraction and the fractional contribution from the amplitude analysis.

Resonance	J^P	$\mathcal{B}(B^- \to R^0\pi^-) \times \mathcal{B}(R^0 \to D^{*+}\pi^-) \times 10^{-4}$	
		This analysis	Belle collaboration
$D_1(2420)$	1^+	$8.42 \pm 0.08 \pm 0.40 \pm 1.40$	
$D_1(2430)$	1^+S	$3.51 \pm 0.06 \pm 0.23 \pm 0.57$	
$D_2^*(2460)$	2^+	$2.08 \pm 0.03 \pm 0.14 \pm 0.34$	$1.8 \pm 0.3 \pm 0.3 \pm 0.2$
$D_0(2550)$	0^-	$0.72 \pm 0.01 \pm 0.07 \pm 0.12$	
$D_1^*(2600)$	1^-	$0.68 \pm 0.01 \pm 0.07 \pm 0.11$	
$D_2(2740)$	2^-	$0.33 \pm 0.02 \pm 0.14 \pm 0.05$	
$D_3^*(2750)$	3^-	$0.11 \pm 0.01 \pm 0.02 \pm 0.02$	
D_1	1^+	$7.95 \pm 0.09 \pm 0.34 \pm 1.30$	$6.8 \pm 0.7 \pm 1.3 \pm 0.3$
D_1'	1^+	$2.96 \pm 0.30 \pm 0.41 \pm 0.48$	$5.0 \pm 0.4 \pm 1.0 \pm 0.4$

- Comparison with Belle measurements are shown
- Third uncertainty due to absolute measurement of $\mathcal{B}(B^- \to D^{*+}\pi^-\pi^-)$

The $B^- \to D^{*+}\pi^-\pi^-$ Amplitude Analysis

Summary

- A four body amplitude analysis in the $B^- \to D^{*+}\pi^-\pi^-$ decay is performed using *pp* data collected by the LHCb detector
- Fractional contributions and relative phases for resonances contributions are measured
- The data allow for several quasi-model-independent searches for the presence of new states
- Quantum numbers, parameters and branching fractions are measured for $D_1(2420)$, $D_1(2430)$, $D_0(2550)$, $D_1^*(2600)$, $D_2(2740)$ and $D_3^*(2750)$ resonances.
- The $J^P = 1^+S$ and $J^P = 0^-$ QMI amplitudes give indication for the presences of D_1 and $D_0^{'}$ resonances in the 2.80 GeV mass region.
- The data is fitted allowing for mixing between D_1 ad $D_1^{'}$ resonances. The mixing angle deviates from zero by 2.3 σ.

- **Amplitude analysis of $B^+ \to D^+ D^- K^+$ decays**
  - $\mathcal{L} = 9\ \mathrm{fb}^{-1}$, run I 2011 + 2012 and run II 2015 to 2018 data , Phys. Rev. D102 (2020) 112003

- **Model-independent studies of $B^+ \to D^+ D^- K^+$ decays**
  - $\mathcal{L} = 9\ \mathrm{fb}^{-1}$, run I 2011 + 2012 and run II 2015 to 2018 data , Phys. Rev. Lett. 125 (2020) 242001

Amplitude analysis and model-independent studies of $B^+ \to D^+ D^- K^+$ decays

- The $B^+ \to D^{(*)+} D^{(*)-} K^+$ family of decays offers a good laboratory to study charmonium states.

- Branching fractions measurement have been performed $\to$ Recent results by LHCb; but not prior analysis to their resonant structure exist.

$B^+ \to D^+ D^- K^+$ provides a clean environment to study charmonium states:

Resonances in the $D^- K^+$ system:
$\bar{c}d\bar{s}u$ minimal quark content

For the $D^+ K^+$ states ($c\bar{d}\bar{s}u$)

Would indicate exotic contribution

- **With unprecedented pure sample obtained by LHCb the first $B^+ \to D^+ D^- K^+$ amplitude analysis is presented**

- **A model-independent analysis is performed to study the resonant structures in the $D^+ D^-$ channel**

Amplitude analysis and model-independent studies of $B^+ \to D^+ D^- K^+$ decays

- Data sample of 9 fb^{-1}, Full run I + run II data
- B reconstructed as $B^+ \to (K^- \pi^+ \pi^+)_{D^+} (K^+ \pi^- \pi^-)_{D^-} K^+$

- After selection criteria, an extended maximum likelihood fit is applied to $m(D^+ D^- K^+)$ invariant mass

Results:

Phys. Rev. D102 (2020) 112003

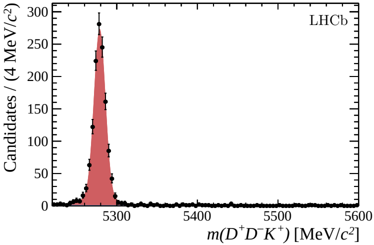

Year	Signal	Background
2011	84 ± 9	—
2012	217 ± 15	16 ± 5
2015	41 ± 6	—
2016	300 ± 18	19 ± 6
2017	302 ± 18	21 ± 6
2018	359 ± 19	15 ± 5

⋆ Total of 1374 candidates

⋆ Signal window: $|m(B^+ - 5280)| < 20$ MeV/c^2

⋆ 1260 candidates, **purity > 99.5%**

Amplitude analysis and model-independent studies of $B^+ \to D^+ D^- K^+$ decays

The projection of candidates in Dalitz plot for the signal window (run II data)

Phys. Rev. D102 (2020) 112003

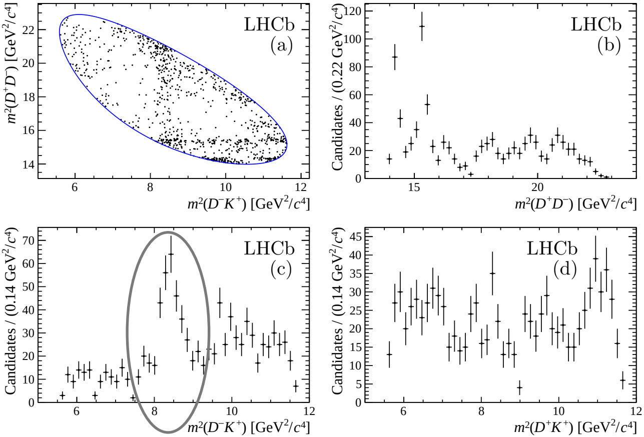

- Data projection of each system
- Clear excess at ≈ 8.25 GeV$^2/c^4$ (also observed for run I data) in D^-K^+.

Strategy

The distribution of $B^+ \to D^+D^-K^+$ events across the Dalitz plot is fitted using a PDF with signal and background contributions and as function of the B phase space.

The signal PDF is defined as:

$$\mathcal{P}_{\text{sig}}(\vec{x}) = \frac{1}{\mathcal{N}} \times \epsilon_{\text{total}}(\vec{x}) \times |\mathcal{A}_{\text{sig}}(\vec{x})|^2$$

$\mathcal{N}$ is a normalization factor
$\epsilon(\vec{x})$ is the total efficiency
$\vec{x}$ position in the Dalitz plot

The signal amplitude $(\mathcal{A}_{sig}(\vec{x}))$ is constructed using the isobar formalism

$$\mathcal{A}_{sig}(\vec{x}) = \Sigma c_j F_j(\vec{x})$$

c_j are the coupling coefficient
$F_j(\vec{x})$ dynamic information of each component.

Signal model content

Strategy I

- Expect only charmonium resonance in D^+D^-
- Expect natural J^P to pseudoscalars and suppressed high-spin

Signal model content: excluding $D^- K^+$ resonances

Strategy I

Phys. Rev. D102 (2020) 112003

- Not excluded possible spin-0 contribution to $\chi_{c2}(3930)$
- m and Γ of $\psi(3770)$, $\psi(4040)$, $\psi(4160)$, $\psi(4415)$ allowed to float
- An exponential S-wave included in the $D^- K^+$ system
  - nonresonant component

- components included in model

(Parameter as given by the PDG)

Partial wave (J^{PC})	Resonance	Mass (MeV/c^2)	Width (MeV)
S wave (0^{++})	$\chi_{c0}(3860)$	3862 ± 43	201 ± 145
	$X(3915)$	3918.4 ± 1.9	20 ± 5
P wave (1^{--})	$\psi(3770)$	3778.1 ± 0.9	27.2 ± 1.0
	$\psi(4040)$	4039 ± 1	80 ± 10
	$\psi(4160)$	4191 ± 5	70 ± 10
	$\psi(4260)$	4230 ± 8	55 ± 19
	$\psi(4415)$	4421 ± 4	62 ± 20
D wave (2^{++})	$\chi_{c2}(3930)$	3921.9 ± 0.6	36.6 ± 2.1
F wave (3^{--})	$X(3842)$	3842.71 ± 0.20	2.79 ± 0.62

$\psi(3770)$ mass and $\chi_{c2}(3930)$ and $X(3842)$ mass and width taken from JHEP 1907 (2019) 035

Results

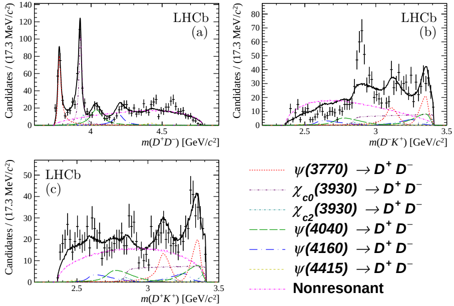

- $\psi(3770)$ taken as reference
- Better fit adding '$\chi_{c0}(3930)$'
- No constraint on '$\chi_{cJ}(3930)$' mass and width

Clear disagreement at $m(D^- K^+) \approx$ 2.9 GeV/c^2

Signal model content: including $D^- K^+$ resonances

Doing a zoom ($m(D^+D^-)$ >4 GeV/c^2)

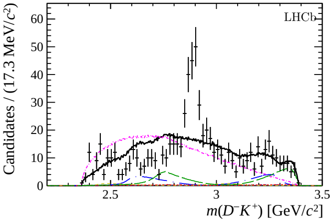

$\Rightarrow$ Clear indication of necessity to include resonant structures in $m(D^- K^+)$

Phys. Rev. D102 (2020) 112003

Strategy II

Constructing a baseline model (adding $D^- K^+$ resonances)

- Adding resonance contributions to better describe the data
- **Best fit when adding a spin-0 and spin-1 $D^- K^+$ resonance**
- The spin-0 and spin-1 $D^- K^+$ contributions are labeled as $X_0(2900)$ **and** $X_1(2900)$
- But no exclusion of the possibility of hadronic effects: such as rescattering
  - Testing this hypothesis require new theoretical models
  - Larger data samples

Signal model content: including D^-K^+ resonances

Phys. Rev. D102 (2020) 112003

- Nonresonant contribution still needed in the D^-K^+ system
- The $D\bar{D}$ structure at $\chi_{cJ}(3930)$ region → **found indeed that spin-0 and spin-2 contributions are necessary**

Baseline model

Resonance	Magnitude	Phase (rad)	Fit fraction (%)
D^+D^- resonances			
$\psi(3770)$	1 (fixed)	0 (fixed)	14.5 ± 1.2 ± 0.8
$\chi_{c0}(3930)$	0.51 ± 0.06 ± 0.02	2.16 ± 0.18 ± 0.03	3.7 ± 0.9 ± 0.2
$\chi_{c2}(3930)$	0.70 ± 0.06 ± 0.01	0.83 ± 0.17 ± 0.13	7.2 ± 1.2 ± 0.3
$\psi(4040)$	0.59 ± 0.08 ± 0.04	1.42 ± 0.18 ± 0.08	5.0 ± 1.3 ± 0.4
$\psi(4160)$	0.67 ± 0.08 ± 0.05	0.90 ± 0.23 ± 0.09	6.6 ± 1.5 ± 1.2
$\psi(4415)$	0.80 ± 0.08 ± 0.06	−1.46 ± 0.20 ± 0.09	9.2 ± 1.4 ± 1.5
D^-K^+ resonances			
$X_0(2900)$	0.62 ± 0.08 ± 0.03	1.09 ± 0.19 ± 0.10	5.6 ± 1.4 ± 0.5
$X_1(2900)$	1.45 ± 0.09 ± 0.03	0.37 ± 0.10 ± 0.05	30.6 ± 2.4 ± 2.1
Nonresonant	1.29 ± 0.09 ± 0.04	−2.41 ± 0.12 ± 0.51	24.2 ± 2.2 ± 0.5

Parameters for $\chi_{c0,2}(3930)$ and $X_{c0,1}(2900)$ determined from the fit

Resonance	Mass (GeV/c^2)	Width (MeV)
$\chi_{c0}(3930)$	3.9238 ± 0.0015 ± 0.0004	17.4 ± 5.1 ± 0.8
$\chi_{c2}(3930)$	3.9268 ± 0.0024 ± 0.0008	34.2 ± 6.6 ± 1.1
$X_0(2900)$	2.866 ± 0.007 ± 0.002	57 ± 12 ± 4
$X_1(2900)$	2.904 ± 0.005 ± 0.001	110 ± 11 ± 4

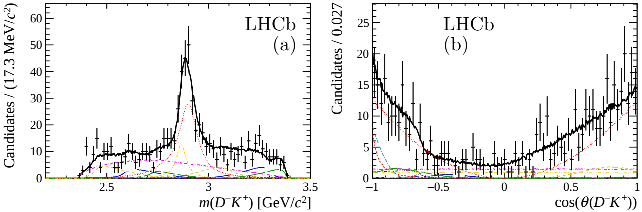

Results

Projections in the $\chi_{cJ}(3930)$ region (Phys. Rev. D102 (2020) 112003)

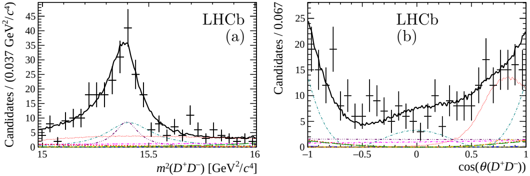

Significance of resonant structures

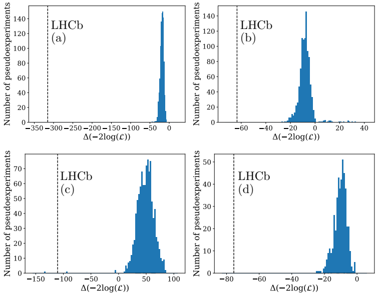

Test t = -2(log($\mathcal{L}(H_1)$) - log($\mathcal{L}(H_0)$))

H_0: Model with no $D^- K^+$ resonances

H_1: Baseline fit model

Dashed line: values found in data

a) H_0: Model with no $D^- K^+$ resonances,
H_1: Baseline fit model
favoured the H1 hypothesis

b), *c*), *d*) H_0: Model with single $\chi_{c0,1,2}$ resonances
H_1 fit model with resonance or both, spin-0 and spin-2

Favoured to spin-0 and spin-2 combination

Model-independent studies of $B^+ \to D^+ D^- K^+$ decays

- Consider the distribution of the cosine of D^+D^- helicity angle ($h(D^+D^-)$) in terms of Legendre Polynomials
- Decomposition in slices of $m(D^+D^-)$

Coefficient in the expansion: $\langle Y_k^j \rangle = \Sigma w_l P_k(h_l(D^+D^-))$ (k-th unnormalised moment)

Phys. Rev. Lett. 125 (2020) 242001

Truncate expansion up to spin-2 ($k_{max} = 4$)

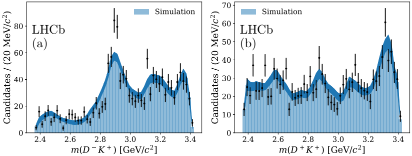

Clear discrepancy around $m(D^-K^+) = 2.9$ GeV/c^2

Construct PDF in $m(D^+D^-)$ to build a test-statistic

$$t = -2 \sum_{l=1}^{N^{\text{Data}}} s_l \log \left(\frac{\mathcal{P}\left(m_l(D^-K^+)|H_0\right)/I_{H_0}}{\mathcal{P}\left(m_l(D^-K^+)|H_1\right)/I_{H_1}} \right)$$

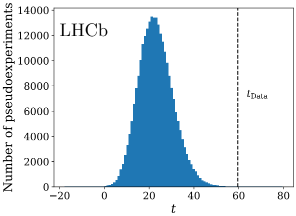

Hypothesis that only D^+D^- resonances up to spin-2 are present is rejected at the 99.99%, (3.9 σ)

Summary

- **First amplitude analysis for the decay channel $B^+ \to D^+ D^- K^+$**
- Dalitz plot distribution cannot be explained using only resonance in the $D^+ D^-$ system
  - Conclusion supported by a model-independent analysis
- Good data description by including new spin-0 and spin-1 resonance in the $D^- K^+$ channel:

  $X_0(2900)$: m $= 2.866 \pm 0.007 \pm 0.002$ GeV$/c^2$, $\Gamma = 57 \pm 12 \pm 4$ MeV
  $X_1(2900)$: m $= 2.904 \pm 0.005 \pm 0.001$ GeV$/c^2$, $\Gamma = 110 \pm 11 \pm 4$ MeV
- **This constitute the first observation of exotic hadron with open flavour**
- It was found necessary to include both spin-0 and spin-2 states in the $\chi_{cJ}(3930)$ region

  $\chi_{c0}(3930)$: m $= 3.9238 \pm 0.0015 \pm 0.0004$ GeV$/c^2$, $\Gamma = 17.4 \pm 5.1 \pm 0.8$ MeV
  $\chi_{c2}(3930)$: m $= 3.9268 \pm 0.0024 \pm 0.0008$ GeV$/c^2$, $\Gamma = 34.2 \pm 6.6 \pm 1.1$ MeV

Final comments

- A lot of work ongoing at the LHCb experiment in the exploration of b and c data
- Great potentiality in the study of charm spectroscopy from B decays
- High expectation for the Run 3 and an upgraded LHCb detector: exciting prospects for further discoveries in this area.

BACK UP

Dalitz plot

⋆ The Dalitz plot (DP) is a tool widely used in the study of three-body decays.

⋆ It is the representation of the phase space of a decay.

⋆ It can be defined in terms of two out of three following invariants:

$$m_{12}^2 = (p_1 + p_2)^2,$$
$$m_{13}^2 = (p_1 + p_3)^2,$$
$$m_{23}^2 = (p_2 + p_3)^2.$$

⋆ The event distribution in Dalitz plot is proportional to the square of the decay amplitude.

$$d\Gamma = \frac{1}{256\pi^3 M^3} |A|^2 dm_{ij}^2 dm_{ik}^2,$$

⋆ Being so, any non-uniform distribution of points in the Dalitz plot directly reflects the dynamic in the decay.

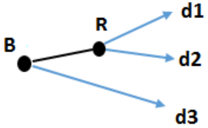

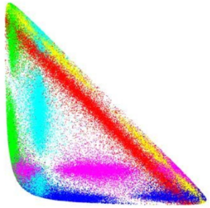

The $B^- \to D^{*+}\pi^-\pi^-$ Amplitude Analysis

Angles definition to distinguish between different J^P contributions:

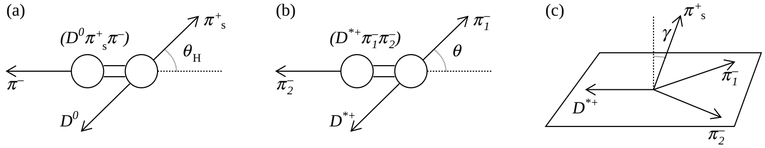

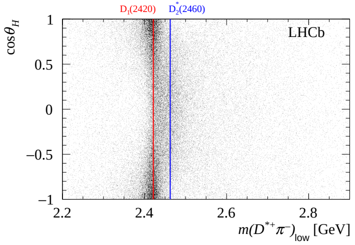

- θ_H is useful in discriminating between natural and unnatural spin-parity resonance.
- Two dimensional distribution of $\cos(\theta_H)$ vs $m(D^{*+}\pi^-)_{low}$

The two vertical lines are due to $D_1(2420)$ and $D_2^*(2462)$ (follow the $1 - hcos^2(\theta_H)$ and $sin^2(\theta_H)$ distribution respectively.
$h < 1$ depends on the properties of the decay.

The $B^- \to D^*\pi^-\pi^-$ Amplitude Analysis

Quasi-Model-Independent amplitude

QMI used to describe broad $J^P = 1^+S$ amplitudes and to search for additional resonances.

- The $D^{*+}\pi^-$ spectrum is divided in 31 slices with nonuniform bin widths.
- The fit is performed using as free parameters the real and imaginary parts of the amplitude in each bin.
- $J^P = 1^+D$ narrow amplitude is taken as reference
- To search for QMI parameters is performed using random search and QMI amplitudes are introduced one by one.
- A second interaction was started from final values of the first fit.
- The fit converges at the second iteration giving positive covariance matrix

Determination of quantum numbers for several excited charmed mesons observed in $B^- \to D^{*+}\pi^-\pi^-$

Measured parameters and quantum numbers in this analysis vs other analysis/experiments

Resonance	J^P	Decays	Mass [MeV]	Width [MeV]	References
$D_0(2550)^0$	0^-	$D^{*+}\pi^-$	$2518 \pm 2 \pm 7$	$199 \pm 5 \pm 17$	This work
$D_J(2550)^0$		$D^{*+}\pi^-$	$2539.4 \pm 4.5 \pm 6.8$	$130 \pm 12 \pm 13$	BaBar [11]
$D_J(2580)^0$		$D^{*+}\pi^-$	$2579.5 \pm 3.4 \pm 3.5$	$177.5 \pm 17.8 \pm 46.0$	LHCb [12]
$D_1^*(2600)^0$	1^-	$D^{*+}\pi^-$	$2641.9 \pm 1.8 \pm 4.5$	$149 \pm 4 \pm 20$	This work
$D_J^*(2600)^0$		$D^+\pi^-$	$2608.7 \pm 2.4 \pm 2.5$	$93 \pm 6 \pm 13$	BaBar [11]
$D_J^*(2650)^0$		$D^{*+}\pi^-$	$2649.2 \pm 3.5 \pm 3.5$	$140.2 \pm 17.1 \pm 18.6$	LHCb [12]
$D_1^*(2680)^0$		$D^+\pi^-$	$2681.1 \pm 5.6 \pm 4.9$	$186.7 \pm 8.5 \pm 8.6$	LHCb [14]
$D_2(2740)^0$	2^-	$D^{*+}\pi^-$	$2751 \pm 3 \pm 7$	$102 \pm 6 \pm 26$	This work
$D_J(2750)^0$		$D^{*+}\pi^-$	$2752.4 \pm 1.7 \pm 2.7$	$71 \pm 6 \pm 11$	BaBar [11]
$D_J(2740)^0$		$D^{*+}\pi^-$	$2737.0 \pm 3.5 \pm 11.2$	$73.2 \pm 13.4 \pm 25.0$	LHCb [12]
$D_3^*(2750)^0$	3^-	$D^{*+}\pi^-$	$2753 \pm 4 \pm 6$	$66 \pm 10 \pm 14$	This work
$D_J^*(2760)^0$		$D^{*+}\pi^-$	$2761.1 \pm 5.1 \pm 6.5$	$74.4 \pm 3.4 \pm 37.0$	LHCb [12]
		$D^+\pi^-$	$2760.1 \pm 1.1 \pm 3.7$	$74.4 \pm 3.4 \pm 19.1$	LHCb [12]
		$D^+\pi^-$	$2763.3 \pm 2.3 \pm 2.3$	$60.9 \pm 5.1 \pm 3.6$	BaBar [11]
$D_J^*(2760)^+$		$D^0\pi^+$	$2771.7 \pm 1.7 \pm 3.8$	$66.7 \pm 6.6 \pm 10.5$	LHCb [12]
$D_3^*(2760)^+$	3^-	$D^0\pi^-$	$2798 \pm 7 \pm 1$	$105 \pm 18 \pm 6$	LHCb [13]
$D_3^*(2760)^0$	3^-	$D^+\pi^-$	$2775.5 \pm 4.5 \pm 4.5$	$95.3 \pm 9.6 \pm 7.9$	LHCb [14]

Fit results from amplitude analysis used for the computation of partial branching fractons

Resonance	J^P	fraction (%)	phase (rad)
$D_1(2420)$	1^+D	$56.5 \pm 0.3 \pm 1.1$	0
$D_1(2430)$	1^+S	$26.0 \pm 0.4 \pm 1.7$	$-1.57 \pm 0.02 \pm 0.08$
$D_2^*(2460)$	2^+	$15.4 \pm 0.2 \pm 0.1$	$-0.77 \pm 0.01 \pm 0.01$
$D_1(2420)$	1^+S	$5.9 \pm 0.5 \pm 2.9$	$1.69 \pm 0.02 \pm 0.06$
$D_0(2550)$	0^-	$5.3 \pm 0.1 \pm 0.5$	$1.50 \pm 0.02 \pm 0.06$
$D_1^*(2600)$	1^-	$5.0 \pm 0.1 \pm 0.5$	$0.76 \pm 0.02 \pm 0.03$
$D_2(2740)$	2^-P	$0.57 \pm 0.07 \pm 0.23$	$-2.14 \pm 0.07 \pm 0.16$
$D_2(2740)$	2^-F	$1.9 \pm 0.1 \pm 1.0$	$0.49 \pm 0.04 \pm 0.40$
$D_3^*(2750)$	3^-	$0.78 \pm 0.06 \pm 0.13$	$-1.54 \pm 0.05 \pm 0.04$
Sum		$117.3 \pm 0.8 \pm 3.8$	